Intestinal Sterol Absorption Mediated by Scavenger Receptors Is Competitively Inhibited by Amphipathic Peptides and Proteins†

Georg Schulthess,*,‡ Sabina Compassi,§ Moritz Werder,§ Chang-Hoon Han,§ Michael C. Phillips,|| and Helmut Hauser*,§

Institute of Biochemistry, Swiss Federal Institute of Technology, ETH Center, Universitätstrasse 16, CH-8092 Zurich, Switzerland, Allegheny University of the Health Sciences, MCP, Hahnemann School of Medicine, Biochemistry Department, 2900 Queen Lane, Philadelphia, Pennsylvania 19129, and Department of Internal Medicine, Medical Policlinic, University Hospital, CH-8091 Zurich, Switzerland

Received May 23, 2000; Revised Manuscript Received August 2, 2000

ABSTRACT: Exchangeable serum apolipoproteins and amphipathic α-helical peptides are effective inhibitors of sterol (free and esterified cholesterol) uptake at the small-intestinal brush border membrane. The minimal structural requirement of an inhibitor is an amphipathic α-helix of 18 amino acids. The inhibition is competitive, indicating that the inhibitor binds to scavenger receptor class B type I (SR-BI) present in the brush border membrane and responsible for sterol uptake. Binding of apolipoprotein A-I to SR-BI of rabbit brush border membrane is cooperative, characterized by a dissociation constant $K_d = 0.45\ \mu M$ and a Hill coefficient of $n = 2.8$. The cooperativity of the interaction is due to binding of the inhibitor molecule to a dimeric or oligomeric form of SR-BI held together by disulfide bridges. Consistent with the competitive nature of the inhibition, the K_d value agrees within experimental error with the IC_{50} value of inhibition and with the inhibition constant K_I. After proteinase K treatment of brush border membrane vesicles, the affinity of the interaction of apolipoprotein A-I expressed as K_d is reduced by a factor of 20, and the cooperativity is lost. The interaction of proteinase K-treated brush border membrane vesicles with apolipoprotein A-I is nonspecific partitioning of the apolipoprotein into the lipid bilayer of brush border membrane vesicles.

Using various in vitro models for the small-intestinal brush border membrane (BBM)[1] such as brush border membrane vesicles (BBMV), intact enterocytes, and Caco-2-cells, we were able to show that sterol absorption by the BBM is an energy-independent, protein-mediated process (*1*−*5*). This finding is at variance with the generally accepted view documented in review articles and text books, that dietary lipids diffuse passively along their concentration gradient from the lumen of the small intestine across the BBM to the cytosol of the epithelial cells. Recently we identified a scavenger receptor of class B type I (SR-BI) as an integral protein of the BBM that is responsible for the facilitated uptake of sterols in the small-intestinal BBM (*7*). We showed that this receptor functions as a lipid port for several classes of dietary lipids including cholesteryl esters, triacylglycerols, and phospholipids.

The physiological ligand of SR-BI in liver and steroidogenic tissue is high-density lipoprotein or, generally speaking, apolipoprotein A-I-containing lipoprotein particles. We are able to show that binding of high-density lipoprotein and apolipoprotein A-I (apo A-I) to BBM-resident SR-BI inhibits the uptake of sterols and other dietary lipids into the small-intestinal BBM (*7*).

In a previous report (*6*), we showed that other exchangeable serum apolipoproteins such as apo A-II and apo A-IV also inhibit sterol uptake, though to a different extent. Evidence was presented to show that the structural motif underlying the inhibition is the amphipathic α-helix (*6*). A peptide of 18 amino acids (18A) forming an ideal amphipathic α-helix of class A was shown to be an effective inhibitor of sterol uptake, while peptide 18S (scrambled 18A), consisting of the same 18 amino acids in a randomized sequence, was inactive (*6*). The randomization of the amino acid sequence apparently abolishes the amphipathic character of the helical peptide. Here we address the question of the mechanism of inhibition of lipid uptake. Evidence is presented to show that inhibitors of lipid uptake such as serum apolipoproteins, serum lipoproteins, and synthetic, amphipathic, α-helical peptides in general are ligands of SR-BI competing successfully with various donor particles for the binding site(s) on SR-BI.

† This work was supported by the Swiss Federal Institute of Technology, the Swiss National Science Foundation (Grants 31-32441.91 and 32-46810.96), NIH Grant HL 22633, and the Kamillo Eisner-Stiftung, CH-6062 Hergiswil and E. M. Warburg, Pincus & Co. International, Ltd.

* To whom correspondence should be addressed. E-mail: helmut.hauser@bc.biol.ethz.ch (H.H.), georg.schulthess@dim.usz.ch (G.S.)

‡ Medical Policlinic, University Hospital.

§ Institute of Biochemistry, Swiss Federal Institute of Technology.

|| Allegheny University of the Health Sciences, Hahnemann School of Medicine.

[1] Abbreviations: apo, apolipoprotein; BBM, brush border membrane(s); BBMV, brush border membrane vesicle(s); BSA, bovine serum albumin; CD, circular dichroism; Doxyl, 4,4-dimethyl-3-oxazolidinyloxy; DTT, 1,4-dithio-*rac*-threitol; HDL, high-density lipoprotein(s); HPLC, high-performance liquid chromatography; PAGE, polyacrylamide gel electrophoresis; PBS, phosphate-buffered saline; PC, phosphatidylcholine; SDS, sodium dodecyl sulfate; SR-BI, scavenger receptor class B, type I; SUV, small unilamellar vesicle(s); Tris, tris(hydroxymethyl)aminomethane; TTBS, Tween 20 in Tris-buffered saline.

10.1021/bi0011633 CCC: $19.00
Published on Web 09/19/2000

MATERIALS AND METHODS

Materials

Egg phosphatidylcholine (PC) and dimyristoyl-PC were purchased from Lipid Products (Nutfield, Surrey, U.K.), cholesterol (purity >99%) from Fluka, cholesteryl oleate (purity >98%), 5-doxylstearic acid, 1-palmitoyl-2-(16-doxylstearoyl)-*sn*-phosphatidylcholine (5-doxyl-PC), and 3-doxyl-5α-cholestane from Sigma (Buchs, Switzerland), Protein G Sepharose from Amersham Pharmacia Biotech (Dübendorf, Switzerland), the Chemiluminescent Kit (Immun-Star) from Bio-Rad (Glattbrugg, Switzerland), monoclonal anti-apo A-I antibody from Pierce (Lausanne, Switzerland), polyclonal antibody against the C-terminal sequence (CSPAAKGTV-LQEAKL) of mouse SR-BI raised in rabbit (pAb I15) from Novus Biologicals Inc. (AbCam, Cambridge, U.K.), [4-^{14}C]-cholesterol (~50 Ci/mol), [1α, 2α(N)-^{3}H]cholesterol (47 Ci/mmol), and [1α, 2α(N)-^{3}H]cholesteryl oleyl ether (37 Ci/mmol) from Amersham (U.K.). The peptides Ac-18A-NH_2 (CH_3CO-DWLKAFYDKVAEKLKEAF-NH_2), Ac-15A-NH_2 (CH_3CO-KAFYDKVAEKLKEAF-NH_2), Ac-12A-NH_2 (CH_3-CO-YDKVAEKLKEAF-NH_2), and Ac-9A-NH_2 (CH_3CO-VAEKLKEAF-NH_2) (*7*−*10*) were all synthesized by solid-phase methods with the N-terminus being acetylated and the C-terminus amidated and supplied by Genosys (Cambridge, U.K.). Ac-18A-NH_2 was also made of D-amino acids (Ac-18A_D-NH_2). The purity of all peptides was better than 95% as assessed by HPLC, and their molecular weights determined by mass spectrometry were consistent with the calculated values.

Methods

Determination of IC_{50} Values for Inhibition of Sterol Uptake. Rates of cholesteryl oleate uptake were measured by incubating BBMV (2 mg of protein/mL) with SUV of egg PC containing 1 mol % cholesteryl oleate and a trace amount of [^{3}H]cholesteryl oleyl ether (0.05 mg of total lipid/mL), both dispersed in Tris buffer (0.05 M Tris-HCl, pH 7.4, 0.15 NaCl, 0.02% NaN_3) in the absence and presence of inhibitor at 23 °C for 20 min. The rate of cholesteryl oleate uptake by BBMV in the absence of inhibitor was taken as 100%, and the reduction in uptake rate measured in the presence of inhibitor was expressed as percent inhibition. This yielded dose−response curves relating percent inhibition to the total inhibitor concentration. The experimental data were fitted by the Hill equation (*11*):

$$\text{inhibition (\%)} = 1/[1 + (IC_{50}/x)^n] \quad (1)$$

where x is the total inhibitor concentration, IC_{50} the inhibitor concentration at which 50% of the inhibition was observed, and n the Hill coefficient. We note that the IC_{50} value is identical to the dissociation constant K_d of the interaction.

Binding of Apo A-I to Rabbit Small-Intestinal BBMV and Protein-Free Lipid Vesicles. The binding of apo A-I to BBMV was determined under the conditions of the lipid uptake measurements. BBMV (2 mg of protein/mL) and egg PC SUV containing 1 mol % [^{3}H]cholesterol (0.05 mg of total lipid/mL) dispersed in Tris buffer were both incubated with increasing quantities of [^{14}C]apo A-I at room temperature for 20 min. BBMV were separated from unbound apo A-I by centrifugation at 115000*g* for 2 min in a Beckman airfuge, and the radiolabeled apo A-I present in the supernatant was determined by counting three aliquots in a Beckman LS-7500 liquid scintillation counter. For comparison, the binding of apo A-I to BBMV after digestion with proteinase K and to large unilamellar vesicles made from the lipid extract of BBMV was measured. The concentrations of the proteinase K-treated BBMV and the large unilamellar vesicles of the lipid extract both dispersed in Tris buffer were 2.6 and 4 mg of total lipid/mL, respectively. The partitioning of human apo A-I into bilayers of egg PC SUV dispersed in Tris buffer was determined by incubating egg PC SUV containing 1 mol % [^{3}H]cholesterol (5 mg of total lipid/mL) with increasing amounts of [^{14}C]apo A-I at room temperature for 20 min. The amount of apo A-I partitioned into egg PC bilayers of SUV was determined by gel filtration on Sepharose CL-4B. The interaction of apo A-I with various vesicles can be treated either as partitioning of the protein between the lipid bilayer and the aqueous phase or as binding of the protein to membrane constituent molecules using the mass action law. The partition coefficient K is calculated as the ratio x_b/x_w from the following equation:

$$K = c_b/(L + c_b)c_w \quad (2)$$

where x_b and x_w are the mole fractions of apo A-I in the vesicle bilayer and the aqueous phase, respectively, c_b is the concentration of apo A-I in the bilayer, c_w is the concentration of free apo A-I, and L is the total lipid concentration. Since the apo A-I concentration in the lipid phase of lipid vesicles or BBMV is small ($c_b \ll L$), eq 2 reduces to

$$c_b/L = Kc_w \quad (3)$$

Equation 3 indicates that the molar ratio of membrane-bound apo A-I to lipid increases linearly with the free apo A-I concentration. Application of the mass action law to the interaction of apo A-I with membrane vesicles yields eq 4 which is the Scatchard equation (*12*, *13*):

$$y/c_w = K_A - yK_A \quad (4)$$

where y is the fraction of total binding sites occupied by apo A-I and $K_A = 1/K_d$ is the binding constant. By substituting for $y = c_b/B_{max}L$, where B_{max} is the number of binding sites per membrane lipid molecule, a Langmuir-type adsorption isotherm is obtained:

$$c_b/L = (B_{max}K_Ac_w)/(1 + K_Ac_w) \quad (5)$$

Gel Filtration. Gel filtration on calibrated Sepharose CL-4B was carried out as described before (*14*, *15*). The column (42 cm × 1 cm) was equilibrated and run at room temperature with Tris buffer. Volumes ranging from 0.3 to 0.6 mL were carefully applied to the top of the gel, and lipids and proteins were eluted from the column with the same buffer at a flow rate of 17 mL/h. The effluent was collected in an LKB fraction collector, and each fraction was analyzed for radioactivity by counting aliquots in a Beckman LS 7500 liquid scintillation counter. The recovery of lipids and proteins was between 85 and 95%. The column void volume $V_0 = 11.4 \pm 0.5$ mL and the total column volume $V_t = 34$

± 0.5 mL were determined by chromatographing dextran blue and $K_3[Fe(CN)_6]$, respectively. Sepharose CL-4B was calibrated as described before (*14*, *15*). Stokes radii, R_h, were calculated from the elution volume V_e according to Ackers (*16*):

$$R_h = a_0 + b_0 \text{ erf}^{-1}(1 - K_e) \quad (6)$$

$$K_e = (V_e - V_0)/(V_t - V_0) \quad (7)$$

where a_0 and b_0 are constants characteristic of the column material. The values derived from the calibration curve are $b_0 = 0 \pm 0.5$ and $b_0 = 18 \pm 1$ if R_h is expressed in nanometers. The chromatograms (gel filtration patterns) were simulated with Gaussian distribution functions using the software Origin (Microcal Software, Inc., Northampton, MA).

Production of Polyclonal Antibodies Raised against Human SR-BI. The C-terminal peptide (CSKKGSKDKEAIQAYSESLMTA) of human SR-BI was synthesized by Genosys (Cambridge, U.K.), and polyclonal antibodies against this peptide were raised in rabbit (pAb 589). The extracellular domain of human SR-BI containing amino acids L41−A421 was produced as a recombinant protein (*7*), and polyclonal antibodies against this portion were raised in goat (pAb 380).

Immunoprecipitations. BBMV (30 mg of protein/mL) were resuspended in 2 mL of lysis buffer (50 mM Tris, pH 8.0, 0.15 M NaCl) containing 1% Triton X-100. After resuspension, the sample was homogenized with 5 strokes of a Dounce homogenizer. The homogenate was microcentrifuged at 14 000 rpm (15800*g*) for 10 min at 4 °C, and the supernatant was incubated with 20 μL of antibody against the extracellular domain of human SR-BI (pAb 380) at 4 °C for 1 h. Protein G Sepharose beads (100 μL of 1:1 slurry) (Amersham) were added, incubated for a further 1 h at 4 °C, and collected by microcentrifugation at 11 000 rpm (10000*g*) for 15 s. Bound immune complexes were washed 3 times with 1 mL of lysis buffer, and twice with 1 mL of PBS, pH 7.4. Immunoprecipitated proteins were eluted by boiling for 5 min in Laemmli sample buffer.

SDS−PAGE and Western Blotting. Denatured samples were microcentrifuged briefly, and supernatants were separated on 7.5% SDS−PAGE and transferred onto a nitrocellulose membrane (Bio-Rad). After blocking with 2% BSA in Tris-buffered saline (50 mM Tris, pH 7.4, 0.15 M NaCl) with 0.05% (v/v) Tween 20 (TTBS), membranes were incubated with primary antibodies at a 1:1000 dilution in TTBS containing 0.2% BSA for more than 1 h. After 4 washes (10 min each), the membranes were incubated for 40 min with an alkaline phosphatase-conjugated secondary antibody (Sigma) at a 1:10 000 dilution in TTBS containing 0.2% BSA. After 4 additional washes in TTBS, the membranes were incubated with a chemiluminescent reagent according to the manufacturer's protocol (Bio-Rad), and were exposed to a Hyperfilm (Amersham).

Preparation of ^{125}I-Apo A-I. ^{125}I-Apo A-I was prepared by incubating 200 μg of human apo A-I in 100 μL of PBS, pH 7.4, with 500 μCi of Na^{125}I (100 μCi/μL, from NEN) for 30 s in an IODO-GEN-precoated iodination tube (from Pierce) at room temperature. The reaction was stopped by transferring the mixture into a new IODO-GEN-precoated iodination tube which includes 18.5 nmol of KI in 10 μL of PBS. The ^{125}I-apo A-I was separated from free radioactivity by passing the reaction mixture through a PD-10 desalting column (Amersham Pharmacia Biotech.) which was pretreated with 1% BSA in PBS and equilibrated with 50 mL of PBS. Fractions of 1 mL were collected, and the radioactivity of 10 μL aliquots was monitored using a gamma counter. The fourth and fifth fractions containing the highest radioactivities were combined (17 ± 4% of recovery yield), and were used for the apo A-I overlay assay.

Apo A-I Overlay Analysis. For the apo A-I binding assay, two identical sets of blotted membranes were prepared. After blocking with 2% of BSA, one set was overlayed with 200 μg of cold apo A-I in 40 mL of TTBS containing 0.2% of BSA for 3−5 h at room temperature. After 4 washes (10 min each), the membrane was incubated with anti apo A-I (monoclonal; Santa Cruz) at a 1:1000 dilution in TTBS containing 0.2% BSA for 1 h. After washing, the membrane was incubated for 40 min with alkaline phosphatase-conjugated anti-mouse IgG at a 1:10 000 dilution in TTBS and processed as described in the Western blotting protocol. Another set was blocked with 2% of BSA and overlayed with 40 μg of ^{125}I-labeled apo A-I in 40 mL of TTBS containing 0.2% BSA for 3−5 h at room temperature. After several washing steps, the membrane was dried in a gel dryer for 30 min at 60 °C, and exposed onto a film overnight.

Miscellaneous. Published methods were used for the preparation of SUV (*1*−*4*) and rabbit small-intestinal BBMV (*3*, *17*), for the digestion of BBMV with proteinase K (*18*), for the extraction of lipids from BBMV (*17*, *19*), for the preparation of human HDL, HDL_3, human apo A-I (*6*), [^{14}C]-apo A-I (3.6 μCi/mg of protein) (*20*), and total apo C (*21*) and its isoforms (apo C-I, C-II, C-III_1, and C-III_2) (*22*), for the isolation and purification of apo E (*21*, *23*), for the reconstitution of discoidal HDL particles from human apo A-I and an unsonicated dimyristoyl-PC dispersion (*24*), and for kinetic measurements of lipid uptake using either bile salt micelles or small unilamellar lipid vesicles as the donor and rabbit intestinal BBMV as the acceptor (*1*−*4*). The purity of lipoproteins and apolipoproteins was checked by agarose gel electrophoresis (*25*) or SDS−PAGE using the Phast Electrophoresis system and 8−25% gradient gels according to the manufacturers' (Pharmacia) recommendations. BBMV were spin-labeled by incubation of BBMV (5 mg of protein/mL, 3 mg of total lipid/mL) with SUV (egg PC and 20 mol % of the spin-label) dispersed in 0.1 mL of Tris buffer at room temperature overnight. After incubation, spin-labeled BBMV were washed 3 times with 1 mL of the same buffer and dispersed in 0.1 mL of Tris buffer, and ESR spectra were recorded as described before (*26*).

Analytical Methods. Phospholipid concentrations (*27*) and protein concentration were determined by published methods (*6*). SDS−PAGE was carried out in a Mini-Protean II dual slab cell from Bio-Rad according to the instruction manual. The molecular mass of the synthetic peptides was determined by matrix-assisted laser desorption ionization mass spectrometry using time-of-flight mass analysis (Voyager Elite mass spectrometry from PerSeptive Biosystem). For curve fitting, the programs MacCurveFit (Kevin Raner Software, Victoria, Australia) and Excel (Microsoft) were used on a Macintosh computer.

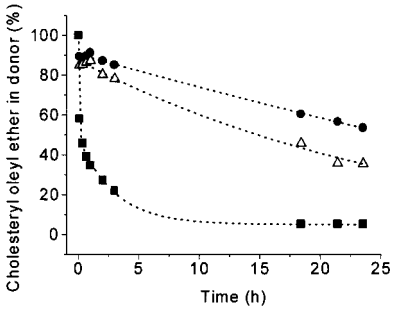

FIGURE 1: Kinetics of cholesteryl ester uptake by rabbit BBMV. SUV of egg PC containing 1 mol % cholesteryl oleate labeled with [^{3}H]cholesteryl oleyl ether (0.05 mg of total lipid/mL) were incubated at room temperature with BBMV (5 mg of protein/mL) in the absence of HDL_3 (■) and in the presence of HDL_3 (50 μg of protein/mL, △; 100 μg of protein/mL, ●). The data points are the average of three different measurements in duplicate. The standard deviations were less than 5%, and the error bars were smaller than the size of the symbols and therefore omitted. The dotted lines were obtained by curve fitting using eq 8.

RESULTS

Kinetics of Sterol Uptake by Rabbit Small-Intestinal BBMV from Small Unilamellar Phospholipid Vesicles (SUV) as the Donor in the Absence and Presence of Inhibitors. Cholesteryl oleate was used as representative of the class of sterols and cholesteryl oleyl ether as a nonhydrolyzable analogue of cholesteryl oleate. The kinetics of cholesteryl oleate uptake by BBMV from SUV as the donor in the absence of inhibitor are shown in Figure 1. The data were adequately fitted by the sum of two exponential functions:

$$x = x_\infty + (x_0 - x_{1\infty})e^{-k_1 t} + (x_{1\infty} - x_\infty)e^{-k_1' t} \qquad (8)$$

where x_0, x, $x_{1\infty}$, and x_∞ represent the fractions or percentages of radiolabel in the donor at time 0, at t, at the end of the first kinetic phase of sterol uptake, and at the final equilibrium, respectively; k_1 and k_1' are the pseudo-first-order rate constants of the first and second phases of sterol uptake, respectively; the preexponential terms $(x_0 - x_{1\infty})$ and $(x_{1\infty} - x_\infty)$ represent the intensities of the first and second exponential decay function, respectively. The kinetic parameters derived from curve fitting using eq 8 are summarized in Table 1. The pseudo-first-order rate constant k_1 (half-time $t_{1/2}$) for the initial fast phase of cholesteryl oleate uptake was $k_1 = 21 \pm 6$ h^{-1} ($t_{1/2} = 2.4 \pm 0.6$ min) and for the second slower phase $k_1' = 0.45 \pm 0.18$ h^{-1} ($t_{1/2} = 1.6 \pm 0.7$ h), consistent with published data (*5*). As had been noticed before (*2*), similar kinetics were observed for both free and esterified cholesterol. The uptake kinetics of free cholesterol were measured under the same conditions as described for Figure 1, and the kinetic parameters derived from curve fitting for the initial fast phase agreed within experimental error with those for cholesteryl oleate uptake (Table 1).

As shown in Figure 1, the addition of HDL_3 reduced the intensity $(x_0 - x_{1\infty})$ of the initial fast phase of cholesteryl ester uptake. The preexponential factor $(x_0 - x_{1\infty})$ was about 10% in the presence of 50 μg of HDL_3 protein/mL (Figure 1) and was abolished altogether at HDL_3 concentrations exceeding 100 μg of protein/mL. The data points collected after 20 min were fitted by a single-exponential decay function, yielding k_1 ($t_{1/2}$) values characteristic of cholesteryl ester uptake in the presence of HDL_3. The values derived from curve fitting were $k_1 = 0.048 \pm 0.004$ h^{-1} ($t_{1/2} = 14 \pm 1$ h) in the presence of 50 μg of HDL_3 protein/mL and $k_1 = 0.026 \pm 0.002$ h^{-1} ($t_{1/2} = 28 \pm 2$ h) in the presence of 100 μg of HDL_3 protein/mL. As described previously (*6*), the effect of HDL_3 on the uptake of free cholesterol was similar to that shown for cholesteryl ester uptake in Figure 1. Previously we showed that different apolipoproteins A and their lipidated forms inhibit sterol uptake (*6*).

The effect of lipid-free apo A-I on cholesteryl ester uptake was similar to that of HDL_3 as reported before (*6*): with increasing concentrations of apo A-I, the initial fast phase of sterol uptake was reduced and eventually abolished. To compare the inhibitory effect of different serum apolipoproteins on cholesteryl oleate uptake, dose−response curves were constructed for each apolipoprotein as described under Methods [cf. (*6*)]. The sigmoidal dose−response curves were fitted by eq 1, and the IC_{50} values derived from curve fitting are compiled in Table 2. It is clear from this table that the inhibitory effect is not specific to apo A-I. Other serum apolipoproteins are also inhibitors of sterol uptake though to a different extent.

It was shown (*6*) that the inhibitory effect is not restricted to the class of exchangeable serum apolipoproteins. The amphipathic peptide Ac-18A-NH_2 consisting of 18 amino acids was also an effective inhibitor of sterol uptake at the BBM with an IC_{50} value of 33 ± 2 μg/mL (~15 μM) (*6*). When Ac-18A-NH_2 was synthesized with D-amino acids, its activity was retained to ~75% (Table 3). However, upon progressive reduction of the chain length from 18 to 9 amino acids by removal of amino acids from the N-terminus, the inhibitory activity dropped off markedly and the inhibitory effect of Ac-9A-NH_2 was zero (Table 3).

Interaction of Apo A-I with BBMV and Egg PC SUV. Control experiments were carried out to show that apo A-I, which is known to have detergent-like activity, binds to BBMV but does not solubilize these vesicles, at least not at concentrations used in this study. BBMV at two different concentrations (0.6 mg of protein/mL and 2 mg of protein/mL) were incubated with increasing concentrations of apo A-I ranging from 0 to 360 μg of protein/mL at room temperature for 20 min. These conditions were comparable to those at which uptake and inhibition experiments were carried out. Light scattering at 400 nm of BBMV dispersions remained unchanged after addition of apo A-I up to 360 μg of protein/mL, indicating that the size and size distribution of BBMV are not affected by the addition of apo A-I (data not shown). We conclude that the inhibitory effect of apo A-I cannot be due to solubilization of BBMV by apo A-I.

When apo A-I interacted with or partitioned into bilayers of egg PC SUV, the average size and size distribution of these vesicles remained unaffected as determined by gel filtration on Sepharose CL-4B. Representative gel filtration patterns of a sonicated dispersion of egg PC SUV containing 1 mol % [^{3}H]cholesterol, a solution of [^{14}C]apo A-I, and a sonicated egg PC dispersion after incubation with [^{14}C]apo A-I are shown in Figure 2. The peaks in the elution profiles were fitted with Gaussian distribution functions (see solid lines in Figure 2), and the elution volumes V_e, peak intensities I, and average hydrodynamic radii derived from these fits are summarized in Table 4. The gel filtration pattern of sonicated egg PC SUV consisted of two peaks: a major one with a peak area of 97.5% at an elution volume $V_e = 21$ mL

Table 1: Kinetics[a] of Sterol Uptake by Rabbit BBMV from Egg PC SUV (0.05 mg of Total Lipid/mL) in the Presence and Absence of Inhibitor

lipid taken up	BBMV(protein) (mg/mL)	HDL_3(protein) (μg/mL)	k_1 (h^{-1})	$t_{1/2}$ (h)	$(x_0 - x_{1\infty})$ (%)	k_1' (h^{-1})	$t_{1/2}'$ (h)	$(x_{1\infty} - x_\infty)$ (%)	x_∞ (%)[b]
cholesterol	5	0	15 ± 3	0.05 ± 0.01	–	–	–	–	0 ± 3
cholesteryl oleate	5	0	21 ± 6	0.04 ± 0.01	41 ± 11	0.45 ± 0.18	1.6 ± 0.7	55 ± 13	3 ± 2
cholesteryl oleate	2	0	9 ± 2	0.08 ± 0.02	39 ± 10	0.17 ± 0.04	4.1 ± 1.0	51 ± 14	16 ± 8
cholesteryl oleate	2	50	–	–	–	0.048 ± 0.004	14 ± 1	–	5 ± 1
cholesteryl oleate	2	100	–	–	–	0.026 ± 0.002	28 ± 2 h	–	5 ± 1

[a] The kinetic parameters are the average ± SD of 3 independent experiments which were fitted independently. The x_∞ values were derived from curve fitting. [b] The values for the final equilibrium x_∞ derived from curve fitting agreed within error of the measurement with the experimental values and the values calculated from the ratio of the sizes of the lipid pools in the donor and acceptor particles: $x_\infty = 3\%$ (for 5 mg of BBM protein/mL) and $x_\infty = 8\%$ (for 2 mg of BBM protein/mL).

Table 2: IC_{50} Values for the Inhibition by Human Apolipoproteins of Cholesteryl Oleate Uptake into Small-Intestinal BBMV[a]

inhibitor	IC_{50} (μg/mL)	IC_{50} (μM)
apo A-I[b]	11 ± 1	0.4 ± 0.04
apo C-I	12 ± 2	1.8 ± 0.4
apo C-II	19 ± 1	2.1 ± 0.1
apo $C\text{-}III_1$	4.8 ± 0.8	0.6 ± 0.1
apo $C\text{-}III_2$	4.2 ± 0.2	0.5 ± 0.1
apo E	95 ± 7	2.9 ± 0.2

[a] The IC_{50} values were determined as described under Methods. [b] The inhibitory effect of apo A-I taken from ref *6* is included for comparison.

Table 3: Inhibition by Synthetic Peptides of Cholesteryl Oleate Uptake into Small-Intestinal BBMV[a]

peptide	inhibition (%)
Ac-18A-NH_2	100 ± 10
Ac-$18A_D$-NH_2	73 ± 5
Ac-15A-NH_2	30 ± 10
Ac-12A-NH_2	12 ± 3
Ac-9A-NH_2	0

[a] The rate of cholesteryl oleate uptake was measured using egg PC SUV containing 1 mol % cholesteryl oleate as the donor (0.05 mg of lipid/mL) and rabbit small-intestinal BBMV (2 mg of protein/mL) as the acceptor. The inhibition was measured in the presence of 80 μg of peptide/mL as described under Methods. The inhibitory effect observed with different peptides was normalized to that of Ac-18A-NH_2 which was taken as 100%. Ac-18A-NH_2 = CH_3CO-DWLKAFYDKVAEK-LKEAF-NH_2; Ac-$18A_D$-NH_2 is the same peptide made of D-amino acids. Peptides designated by letter A have the same amino acid sequence as Ac-18A-NH_2 but differ in the number of amino acids counted from the C-terminus.

corresponding to an average vesicle diameter of 22 ± 1 nm and a minor one with a peak area of 2.5% at the void volume $V_0 = 12.5$ mL corresponding to lipid aggregates larger than about 60 nm (Table 4). Pure human apo A-I was eluted as an asymmetric peak at $V_e = 29.1$ mL with a tailing shoulder. The elution volume $V_e = 29.1$ mL corresponds to an apparent hydrodynamic radius $R_h = 3.7 \pm 0.1$ nm, which is consistent with an apo A-I dimer (*28*, *29*). The shoulder probably represents monomeric apo A-I. The V_e value of this shoulder derived from curve fitting is close to the total volume, and since the Stokes radius obtained from this V_e-value is subject to a large error, a more detailed discussion is not justified. The gel filtration patterns of sonicated egg PC vesicles containing 1 mol % [^{3}H]cholesterol after incubation with [^{14}C]apo A-I at room temperature for 20 min are shown in panels C and D (Figure 2). The pattern of radiolabeled [^{14}C]apo A-I in the presence of egg PC was simulated by the sum of four Gaussian functions (Figure 2D) from which the quantities of free and bound apo A-I, i.e., apo A-I associated with egg PC SUV, were obtained (Table 4). These control experiments indicate that under the conditions of our uptake measurements apo A-I-containing SUV are stable. As shown before (*31*), those SUV transfer or exchange choleterol passively. Under the conditions of the experiment of Figure 2C, 61% of apo A-I was coeluted with egg PC SUV. The amount of bound apo A-I appeared to be correlated to the concentration of egg PC SUV. For instance, at the same apo A-I concentration as in Figure 2C (1.8 μM) but at a 100 times smaller concentration of egg PC SUV (i.e., at 0.05 mg of total lipid/mL), the quantity of apo A-I coeluted with the egg PC SUV was reduced to 1.6% (data not shown). Treating this interaction of apo A-I with egg PC SUV as partitioning of the protein between the lipid bilayer and the aqueous phase using eq 2 yielded a partition coefficient $K = (2.4 \pm 0.1) \times 10^{-2}$ M^{-1}.

To shed light on the mode of interaction of apo A-I with BBMV, the binding isotherm for the interaction of apo A-I with BBMV (Figure 3A) was compared to binding isotherms for the interaction of apo A-I with proteinase K-treated BBMV, large unilamellar vesicles made from the lipid extract of BBMV, and egg PC SUV. Inspection of Figure 3 reveals that the shape of the binding curve for intact BBMV (Figure 3A) is sigmoidal. In contrast, the binding curves for the interaction of apo A-I with proteolytically treated BBMV and protein-free lipid vesicles are hyperbolic (Figure 3B,C). The data points shown in Figure 3A were published before (*7*); however, in the previous report, they were fitted by the hyperbolic function of eq 5. Only the comparison of the data of Figure 3A with other binding isotherms (Figure 3) disclosed the sigmoidal character, and, indeed, the goodness of the fit was significantly improved by using the Hill equation (eq 1) rather than eq 5. This fit yielded a Hill coefficient $n = 2.8$, indicating that the binding of apo A-I to intact BBMV is cooperative.

The binding parameters derived from curve fitting of these isotherms are summarized in Table 5. The affinity of apo A-I expressed as K_d was highest for intact BBMV and decreased markedly (by a factor of about 20) upon digestion of BBMV with proteinase K. The binding parameters describing the partitioning of apo A-I into bilayers of egg PC SUV are $K_d = 1.2 \pm 0.2$ μM and $B_{max} = 18 \pm 3$ μg/mg of lipid. The B_{max} value is equal to 0.5×10^{-3} mol of apo A-I/mol of egg PC, which amounts to 1−2 apo A-I molecules per egg PC vesicle of a hydrodynamic radius of $R_h = 11$ nm (Figure 2A and Table 4). Large unilamellar vesicles made of the lipid extract of BBMV bound about half the amount of apo A-I with about half the affinity relative to the binding

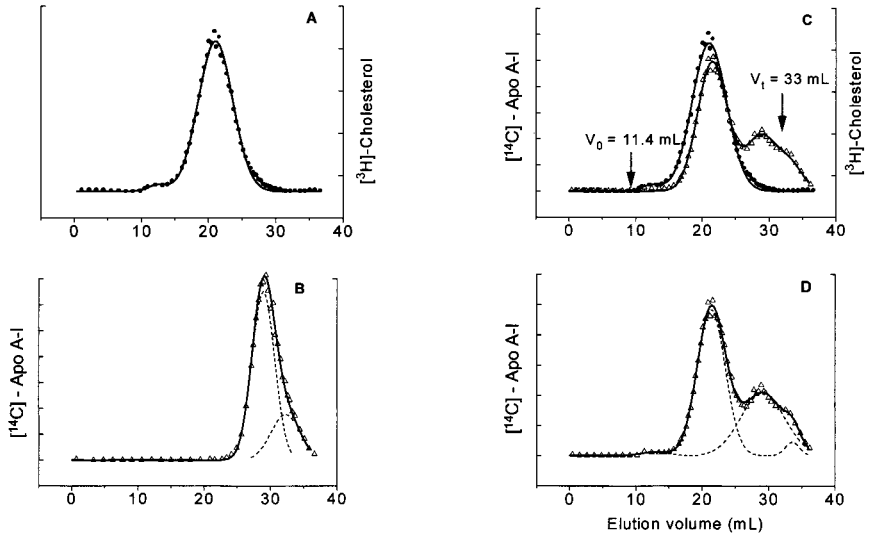

FIGURE 2: Elution profiles obtained by gel filtration on Sepharose CL-4B. Gel filtration patterns of a sonicated dispersion of egg PC containing 1 mol % [^{3}H]cholesterol (5 mg of total lipid/mL) (A), of human [^{14}C]apo A-I (50 μg of protein/mL = 1.8 μM) (B), and of a sonicated egg PC dispersion as in (A) after incubation with [^{14}C]apo A-I (50 μg of protein/mL) at room temperature for 20 min (C). The fractions eluted from the column were analyzed for [^{3}H]cholesterol (●) or [^{14}C]apo A-I (△). The solid lines were obtained by fitting the elution profile with the sum of Gaussian distribution functions. Panel A: the elution pattern of egg PC SUV labeled with [^{3}H]cholesterol (●) was fitted by the sum of two Gaussians. This is also true for egg PC SUV in panel C. Panel B: the asymmetric peak obtained with human apo A-I was fitted by the sum of two Gaussians (dashed curves). Panel D: the gel filtration pattern due to [^{14}C]apo A-I (△) was simulated by four Gaussian functions as shown by the dashed curves.

Table 4: Evaluation of Gel Filtration Patterns (Figure 2) in Terms of Elution Volumes V_e, Peak Intensities I, and Hydrodynamic Radii R_h

particle	peak	elution volume V_e (mL)	peak intensity I (%)	hydrodynamic radius R_h (nm)
egg PC SUV	1	12.5 ± 0.4	2.5	>30
	2	21 ± 0.1	97.5	11 ± 1
apo A-I	1	29.1 ± 0.2	74	3.7 ± 0.1
	2	32 ± 1	26	nd[a]
egg PC SUV	1	12.5 ± 0.6	1.3	>30
and apo A-I	2	21.5 ± 0.1	61.1	11 ± 1
	3	28.9 ± 0.1	29	3.7 ± 0.1
	4	33.4 ± 0.2	8.6	nd

[a] nd = not determined.

of apo A-I to egg PC SUV (Table 5). A comparison of the B_{max} values listed in this table indicates that B_{max} is minimal for apo A-I binding to intact BBMV. The B_{max} value for proteinase K-treated BBMV is about 4 times higher; the B_{max} values obtained with protein-free vesicles are 5−10 times higher than the value for intact BBMV (Table 5).

Western and Apo A-I Overlay Analysis of Native and Immunoprecipitated BBMV. Different anti SR-BI antibodies were raised in different animals against various antigens (see Materials and Methods). Quite unexpectedly, these antibodies detected preferentially different aggregation states of SR-BI in BBMV. For instance, under conditions of short exposure times, antibody pAb 589 detected reproducibly a 140 kDa band (Figure 4A) whereas antibody pAb I15 detected preferentially the 82 kDa band assigned to the glycosylated form of SR-BI. Immunoprecipitation of BBMV solubilized with 1% Triton X-100 was performed with antibody pAb 380 (raised against the extracellular domain of SR-BI). The Western blot analysis of the immunoprecipitate using antibodies pAb 589 and pAb I15 still detected the 140 kDa band (panel A) and the 82 kDa band, respectively. In both native (N) and immunoprecipitated (IP) BBMV, the intensities of the 140 kDa band decreased at high concentration of DTT (lane 2, Figure 4A). In contrast, the intensity of the 82 kDa band increased reproducibly at high DTT concentration (lane 2, Figure 4B). These results suggest that the band at an apparent molecular mass of 140 kDa is probably a dimeric form of SR-BI linked by disulfide bridge(s). However, the data presented cannot discriminate between a homodimer and a heterodimer of SR-BI.

The apo A-I overlay analysis revealed that only the polymeric form of SR-BI binds apo A-I. This is true for native (N) BBMV and immunoprecipitated (IP) BBMV (cf. strips labeled OL/Western, Figure 4C). Minor bands were observed at an apparent molecular mass of 210 kDa, indicating that apo A-I might bind to high-molecular weight polymers of SR-BI (Figure 4C). However, no binding of apo A-I to the monomeric form of SR-BI was detected in the overlay assay.

Nature of the Inhibition of Sterol Uptake in the Presence of Apolipoproteins. To elucidate the nature of the inhibition of sterol uptake by apo A-I, rates (v) of cholesteryl oleate uptake were measured at room temperature as a function of increasing concentrations of cholesteryl oleate in the absence and presence of inhibitor (apo A-I). A plot of the velocities of cholesteryl oleate uptake as a function of substrate concentrations, [S], in the absence of apo A-I yielded typical, hyperbolic saturation curves (Figure 5). The experimental data were adequately fitted by the steady-state version of the Michaelis−Menten rate law:

$$v = V_{max}[S]/(K_m + [S]) \quad (9)$$

where [S] is the substrate concentration equivalent to the concentration of cholesteryl oleate in the donor vesicle, V_{max} is the maximum rate of cholesteryl oleate uptake, and K_m is the Michaelis−Menten constant. Values for V_{max} and K_m derived from curve fitting are listed in Table 6. Figure 5 also shows the rates of cholesteryl oleate uptake in the

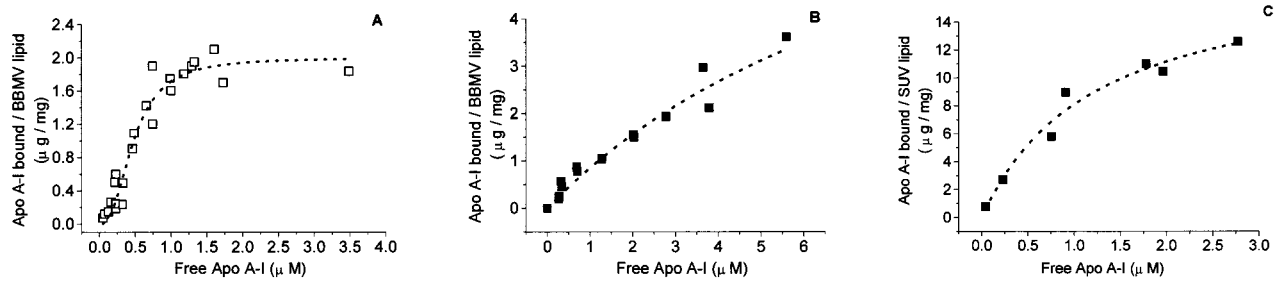

FIGURE 3: (A) Binding isotherm for the interaction of human apo A-I with rabbit intestinal BBMV. The binding isotherm for BBMV was determined under conditions of lipid uptake measurements; i.e., BBMV at 2 mg of protein/mL were incubated in the presence of egg PC SUV containing 1 mol % [^{3}H]cholesterol (0.05 mg of total lipid/mL) with increasing concentrations of [^{14}C]apo A-I at room temperature for 20 min. The amount of apo A-I bound to BBMV was determined as described under Methods, and this amount was plotted as a function of the free apo A-I concentration. The dotted line was obtained by curve fitting using a modified Hill equation (eq 1). (B) Binding isotherm for the interaction of human apo A-I with BBMV subjected to proteinase K treatment (*18*). Experiments were carried out as described for panel A except that the BBMV concentration was 2.6 mg of total lipid/mL and no egg PC vesicles were present. (C) Binding isotherm for the interaction of human apo A-I with egg PC SUV containing 1 mol % [^{3}H]cholesterol. These SUV (5 mg of lipid/mL) were incubated with increasing quantities of [^{14}C]apo A-I at room temperature for 20 min, and the amount of [^{14}C]apo A-I partitioned into the egg PC bilayer was determined by gel filtration on Sepharose CL-4B as described in Figure 2. The dotted line was obtained by curve fitting using eq 5. The data points in panels A−C are the average of two measurements.

Table 5: Isotherms for the Binding of Human Apolipoprotein A-I to Different Vesicles[a]

vesicle	B_{max} (μg/mg of lipid)	K_d (μM)
BBMV	1.9 ± 0.15	0.45 ± 0.05
proteinase K-treated BBMV	7.9 ± 0.3	8.4 ± 1.5
large unilamellar vesicles made from lipid extract of BBMV	10.6 ± 1.5	3.4 ± 1.4
egg PC SUV	18 ± 3	1.2 ± 0.2

[a] B_{max} and K_d values were derived from curve fitting using eq 5 except for the values of intact BBMV which were derived from eq 1. B_{max} values were normalized to the lipid content of the vesicles to allow a direct comparison of the binding properties of different vesicles.

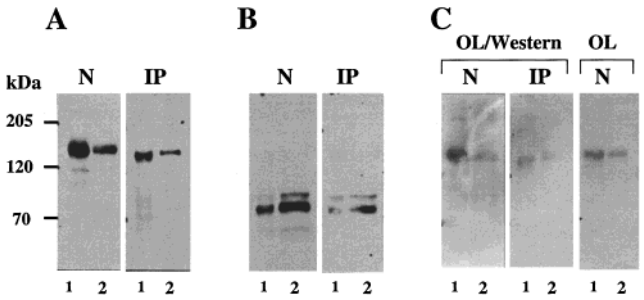

FIGURE 4: Western and apo A-I overlay analysis of native and immunoprecipitated BBMV. Both native BBMV (N) and BBMV immunoprecipitated (IP) with anti-human SR-BI antibody (pAb380; raised in goat) were treated with 1 mM (lane 1) or 100 mM (lane 2) DTT, and were subjected to Western blotting using either anti-SR-BI antibody pAb 589, which specifically detects a 140 kDa band (panel A), or antibody pAb I15, which primarily detects a 82 kDa band (panel B). Panel C shows the apo A-I overlay analysis of native (N) and immunoprecipitated (IP) BBMV. The strips labeled OL/Western were overlayed with cold apo A-I, and bound apo A-I was detected using anti apo A-I antibody as described under Materials and Methods. The strip labeled OL was overlayed with ^{125}I-labeled apo A-I and exposed onto an X-ray film. For comparison sake, equal amounts of protein were applied in lanes 1 and 2 on each strip. Panels A−C are representative of six reproducible experiments in which two different batches of BBMV were used.

presence of 45 and 90 μg/mL apo A-I. The data points obtained in the presence of apo A-I were fitted by eq 9, yielding within experimental error the same value for V_{max} as in the absence of inhibitor but different values for the

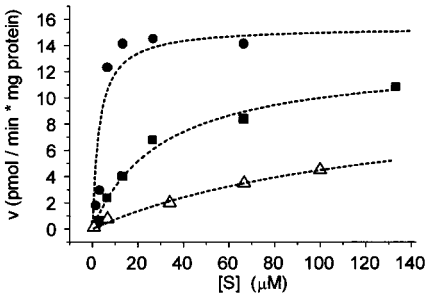

FIGURE 5: Velocities (v) of cholesteryl oleate uptake by BBMV as a function of the substrate concentration, [S], which is the cholesteryl oleate concentration. BBMV at 5 mg of protein/mL were incubated with increasing concentrations of cholesteryl oleate present in donor vesicles at room temperature for 40 min. SUV of egg PC containing 1 mol % cholesteryl oleate trace-labeled with [^{3}H]cholesteryl oleyl ether were used as donor vesicles. Velocities (v) of cholesteryl oleate uptake were measured in the absence of human apo A-I (●) and in the presence of 45 μg of apo A-I/mL (■) and 90 μg of apo A-I/mL (△). The data points are the average of three different measurements, and the standard deviations are less than 5%, i.e., smaller than the size of the symbols.

Table 6: K_m, $K_{m,app}$, and V_{max} Values Derived from Rate Measurements of Cholesteryl Oleate Uptake (Figure 5)

inhibitor (μg/mL)	V_{max} [pmol min^{-1} (mg of protein)$^{-1}$]	K (μM)	K_I (μM)
0	15 ± 1	K_m = 5 ± 1	−
45 (1.61 μM)	14 ± 1	$K_{m,app}$ = 35 ± 4	0.29 ± 0.10
90 (3.21 μM)	12 ± 3	$K_{m,app}$ = 135 ± 50	0.26 ± 0.20

apparent K_m ($K_{m,app}$) (Table 6). This result is characteristic of competitive inhibition for which the Michaelis−Menten constant $K_{m,app}$ is

$$K_{m,app} = K_m(1 + [I]/K_I) \quad (10)$$

where [I] is the inhibitor or apo A-I concentration and K_I is the inhibition constant defined as the dissociation constant for the complex formed between the inhibitor and the enzyme. Lineweaver−Burk transformation of the data of Figure 5 yielded straight-line relations (data not shown); the values for V_{max} and $K_{m,app}$ derived from linear regression analysis are entirely consistent with the values given in Table 6. K_I values derived from the slopes of the Lineweaver−

Burk plots are included in Table 6. We note that these K_I values agree within experimental error with the K_d value derived from the binding of apo A-I to intact BBMV (Table 5).

ESR Spin-Labeling. The above finding that the inhibition by apo A−I is competitive, i.e., that apo A-I interacts directly with the active center(s) of the enzyme, is supported by ESR spin-labeling. ESR spectra were recorded of BBMV spin-labeled with 5-doxylstearic acid, 16-doxyl-PC, and 3-doxyl-5α-cholestane in the absence and presence of apo A-I (50 and 100 μg/mL). For each of the three spin-labels used, superimposable spectra were obtained with and without apo A-I over the time course of the lipid uptake experiment (data not shown). ESR spectra of this kind were published by us before, and we showed that the line shape of these spectra is sensitive to changes in the lipid packing and membrane fluidity (*26*, *30*). The ESR results therefore indicate that the interaction of apo A-I with BBMV has no effect on lipid packing and the fluidity of the BBM. They are consistent with apo A-I interacting with an external surface protein of the BBM.

DISCUSSION

Mechanism of Inhibition of Sterol Uptake. We showed before (*2*) that the kinetics of cholesterol oleate and cholesteryl oleyl ether uptake into small-intestinal BBMV were identical. The advantage of using esterified rather than free cholesterol is that with the more hydrophobic ester there is no contribution from simple passive diffusion to the lipid uptake; i.e., the cholesteryl oleate uptake measured is solely due to the facilitated pathway. Sterol uptake by BBMV is effectively inhibited by apo A-I and its lipidated forms such as HDL_3 (Figure 1, Table 1). The effect of these inhibitors is to reduce the extent of the initial fast phase of sterol uptake expressed as the preexponential term ($x_0 - x_{1\infty}$).

The IC_{50} value for inhibition of sterol uptake by BBMV in the presence of apo A-I is 0.4 ± 0.04 μM (Table 2), and this value agrees within experimental error with the K_d value of 0.45 ± 0.05 μM (Table 5) derived for the binding of apo A-I to BBMV. Remembering that the IC_{50} value is identical to the K_d of the inhibition reaction, the good agreement between the IC_{50} value and the dissociation constant K_d is interpreted to mean that the inhibition is due to binding of apo A-I to the BBM.

The binding of apo A-I to BBMV is distinctly different from the interaction of apo A-I with proteinase K-treated BBMV and protein-free unilamellar lipid vesicles (Figure 3). Characteristic features of the binding of apo A-I to intact BBMV are high affinity and low occupancy as expressed by the values of K_d and B_{max}, respectively (Table 5). Furthermore, the sigmoidal shape of the binding isotherm (Figure 3A) is indicative of cooperative binding. Proteinase K treatment of BBMV abolishes the cooperativity of the apo A-I binding; the shape of the binding isotherm obtained with these vesicles is similar to that of apo A-I partitioning into protein-free lipid bilayers (Figure 3). The affinity of apo A-I binding to proteinase K-treated BBMV is markedly reduced compared to intact BBMV (Table 5). These differences in binding properties between intact BBMV, proteinase K-treated BBMV, and protein-free lipid vesicles (Table 5) can be rationalized by postulating that apo A-I interacts specifically with an integral protein of the BBM. A scavenger receptor (SR-BI) was identified as a candidate protein by our laboratory (*7*). In contrast to native BBMV, the binding of apo A-I to proteolytically treated BBMV and protein-free lipid vesicles is nonspecific, reflecting the partitioning of the protein into the lipid bilayer. The K_d value derived for the partitioning of apo A-I into egg PC bilayers (Table 5) is in good agreement with published data (*32*).

Further information concerning the nature of the interaction of apolipoproteins with the BBM and the mechanism of inhibition is derived from the data presented in Figure 5 and Table 6. These data provide good evidence for the inhibition being competitive: the inhibitor binds reversibly to the enzyme (possibly SR-BI or another member of the family of scavenger receptor) and denies the substrate, i.e., sterols, access to the active site. With the inhibition being competitive, the value of K_I (Table 6) as the K_d for the formation of the inhibitor−enzyme complex is expected to agree within experimental error with the K_d value for apo A-I binding to BBMV (Table 5). This expectation is borne out by experiment (cf. Tables 5 and 6). The good agreement between the IC_{50} value, the dissociation constant K_d, and the inhibition constant K_I lends support to the notion that lipoproteins and apolipoproteins bind to SR-BI and this interaction leads to the inhibition of the facilitated sterol uptake.

Our main conclusion that serum apolipoproteins and lipoproteins as inhibitors of small-intestinal lipid uptake interact directly with SR-BI is consistent with published data. Both apo A-I and HDL have been shown to be physiological ligands of SR-BI (*33*−*37*). The K_d value of 0.45 ± 0.05 μM derived from the binding isotherm (Figure 3A) is of the same order of magnitude as the K_d values obtained for the binding of HDL to the plasma membrane of different cells transfected with either human or murine SR-BI (*35*, *37*).

Our interpretation that the inhibitory effect of apo A-I is due to the direct interaction of apo A-I with scavenger receptors and not to an indirect effect is supported by ESR spin-labeling. The ESR data indicate that the interaction of apo A-I with BBMV does not affect the lipid packing and the membrane fluidity. They are consistent with apo A-I interacting with an external surface domain of an integral protein of the BBM. SR-BI has been described as such a protein. It has two putative anchoring domains: one at the N-terminus and another one at the C-terminus, with most of its mass being exposed at the external membrane surface (*33*, *38*). Binding of apo A-I to SR-BI at the BBM surface is largely reversible. Extensive washing of BBMV, to which apo A-I had been bound and which as a result of this binding had lost their protein-facilitated sterol uptake,was shown to restore the capacity of protein-mediated sterol uptake to 80−90% (*6*). The Western and apo A-I overlay analyses shed light on the origin of the cooperativity of apo A-I binding to SR-BI. The cooperativity could be due to several ligand binding sites per SR-BI molecule or alternatively to apo A-I binding to SR-BI oligomers. The data in Figures 3A and 4 are consistent with the latter case supporting the notion that SR-BI probably functions as a dimer or oligomer linked together by disulfide bridge(s).

Minimum Structural Requirements of an Inhibitor of Sterol Uptake. The data in Table 2 demonstrate that all exchangeable apolipoproteins inhibit sterol uptake, albeit to a different

extent. On a molar basis, two subfractions of apo C, apo C-III_1 and apo C-III_2, are the most effective inhibitors of sterol uptake.

The amphipathic α-helix is the secondary structure motif (*9*, *39*) that is common to all inhibitors listed in Tables 2 and 3. Evidence was presented before to show that the amphipathic α-helix is indeed the structural principle underlying the inhibition (*6*). The minimum structural requirement is an amphipathic α-helix of 18 amino acids. Reducing the chain length to 15 and less amino acids is accompanied by loss of inhibitory activity (Table 3). The helix handedness is not so critical since Ac-18_D-NH_2 forming a left-handed α-helix is almost as active as its L-amino acid analogue (Table 3).

CD measurements showed that both Ac-18A-NH_2 and its D analogue undergo broad, concentration-dependent coil-to-α-helix transitions with a midpoint of about 100 μM. In contrast, the CD spectra of all shorter peptides were indicative of a random-coil conformation up to at least 100 μM (unpublished observation). So the propensity of these peptides of forming an α-helix appears to be correlated to the inhibitory activity.

Physiological Significance. The identification of specific inhibitors of sterol and lipid uptake in the intestinal BBM raises the intriguing possibility of regulating this process. The minimum structural requirement of such an inhibitor has been identified as a short, amphipathic α-helix (*6*). A future generation of inhibitors can be envisaged comprising synthetic, protein-mimetic compounds targeted to SR-BI of the BBM. Such an approach involves the systematic search for inhibitors of SR-BI by high through-put screening methods using appropriate BBM models.

ACKNOWLEDGMENT

We thank Professor Gottfried Schatz for valuable discussions and comments, and Mr. A. Tchouboukov for expert technical assistance. We are indebted to Dr. R. Thomas for communicating the CD results.

REFERENCES

1. Thurnhofer, H., and Hauser, H. (1990) *Biochemistry 29*, 2142−2148.
2. Compassi, S., Werder, M., Boffelli, D., Weber, F. E., Hauser, H., and Schulthess, G. (1995) *Biochemistry 34*, 16473−16482.
3. Schulthess, G., Compassi, S., Boffelli, D., Werder, M., Weber, F. E., and Hauser, H. (1996) *J. Lipid Res. 37*, 2405−2419.
4. Compassi, S., Werder, M., Weber, F. E., Boffelli, D., Hauser, H., and Schulthess, G. (1997) *Biochemistry 36*, 6643−6652.
5. Boffelli, D., Weber, F. E., Compassi, S., Werder, M., Schulthess, G., and Hauser, H. (1997) *Biochemistry 36*, 10784−10792.
6. Boffelli, D., Compassi, S., Werder, M., Weber, F. E., Phillips, M. C., Schulthess, G., and Hauser, H. (1997) *FEBS Lett. 411*, 7−11.
7. Hauser, H., Dyer, J. H., Nandy, A., Vega, M. A., Werder, M., Bieliauskaite, E., Weber, F. E., Compassi, S., Gemperli, A., Boffelli, D., Wehrli, E., Schulthess, G., and Phillips, M. C. (1998) *Biochemistry 37*, 17843−17850.
8. Anantharamaiah, G. M. (1986) *Methods Enzymol. 128*, 627−647.
9. Venkatachalapathi, Y. V., Phillips, M. C., Epand, R. M., Epand, R. F., Tytler, E. M., Segrest, J. P., and Anantharamaiah, G. M. (1993) *Proteins: Struct., Funct., Genet. 15*, 349−359.
10. Yancey, P. G., Bielicki, J. K., Johnson, W. J., Lund-Katz, S., Palgunachari, M. N., Anantharamaiah, G. M., Segrest, J. P., Phillips, M. C., and Rothblat, G. H. (1995) *Biochemistry 34*, 7955−7965.
11. Rodbard, D., and Frazier, G. R. (1975) *Methods Enzymol. 37*, 3−22.
12. Scatchard, G. (1949) *Ann. N.Y. Acad. Sci. 51*, 660−672.
13. Cantor, C. R., and Schimmel, P. R. in *Biophysical Chemistry*, Part III, pp 852−856, W. H. Freeman, San Francisco.
14. Brunner, J., Skrabal, P., and Hauser, H. (1976) *Biochim. Biophys. Acta 455*, 322−331.
15. Schurtenberger, P., and Hauser, H. (1984) *Biochim. Biophys. Acta 778*, 470−480.
16. Ackers, G. K. (1967) *J. Biol. Chem. 242*, 3237−3238.
17. Hauser, H., Howell, K., Dawson, R. M. C., and Bowyer, D. E. (1980) *Biochim. Biophys. Acta 602*, 567−577.
18. Thurnhofer, H., and Hauser, H. (1990) *Biochim. Biophys. Acta 1024*, 249−262.
19. Bligh, E. G., and Dyer, W. J. (1959) *Can. J. Biochem. Physiol. 37*, 911−917.
20. Phillips, M. C., and Krebs, K. E. (1986) *Methods Enzymol. 128*, 387−403.
21. Rall, S. C., Jr., Weisgraber, K. H., and Mahley, R. W. (1986) *Methods Enzymol. 128*, 273−287.
22. Jackson, R. L., and Holdsworth, G. (1986) *Methods Enzymol. 128*, 288−297.
23. Weisgraber, K. H., and Mahley, R. W. (1986) *Methods Enzymol. 129*, 145−166.
24. Brouillette, C. G., and Anantharamaiah, G. M. (1995) *Biochim. Biophys. Acta 1256*, 103−129.
25. Noble, R. P. (1968) *J. Lipid Res. 9*, 693−700.
26. Hauser, H., Gains, N., Semenza, G., and Spiess, M. (1982) *Biochemistry 21*, 5621−5628.
27. Chen, P. S., Jr., Toribara, T. Y., and Warner, H. (1956) *Anal. Chem. 28*, 1756−1758.
28. Donovan, J. M., Benedek, G. B., and Carey, M. C. (1987) *Biochemistry 26*, 8116−8125.
29. Morrisett, J. D., Jackson, R. L., and Gotto, A. M., Jr. (1977) *Biochim. Biophys. Acta 472*, 93−133.
30. Mütsch, B., Gains, N., and Hauser, H. (1986) *Biochemistry 25*, 2134−2140.
31. Letizia, J. Y., and Phillips, M. C. (1991) *Biochemistry 30*, 866−873.
32. Yokoyama, S., Fukushima, D., Kupferberg, J. P., Kezdy, F., and Kaiser, E. T. (1980) *J. Biol. Chem. 255*, 7333−7339.
33. Rigotto, A., Trigatti, B., Babitt, J., Penman, M., Xu, S., and Krieger, M. (1997) *Curr. Opin. Lipidol. 8*, 181−188.
34. Calvo, D., Gomez-Coronado, D., Lasuncion, M. A., and Vega, M. A. (1997) *Arterioscler. Thromb. Vasc. Biol. 17*, 2341−2349.
35. Acton, S., Rigotti, A., Landschulz, K. T., Xu, S., Hobbs, H. H., and Krieger, M. (1996) *Science 271*, 518−520.
36. Xu, S., Laccotripe, M., Huang, X., Rigotti, A., Zannis, V. I., and Krieger, M. (1997) *J. Lipid Res. 38*, 1289−1298.
37. Murao, K., Terpstra, V., Green, S. R., Kondratenko, N., Steinberg, D., and Quehenberger, O. (1997) *J. Biol. Chem. 272*, 17551−17557.
38. Vega, M. A., Segui-Real, B., Garcia, J. A., Cales, C., Rodriguez, F., Vanderkerckhove, J., and Sandoval, I. V. (1991) *J. Biol. Chem. 266*, 16818−16824.
39. Segrest, J. P., Garber, D. W., Brouillette, C. G., Harvey, S. C., and Anantharamaiah, G. M. (1994) *Adv. Protein Chem. 45*, 303−306.

BI0011633